



The ‘Sticky Elastica’: Delamination blisters beyond small deformations

by

**Till J. W. Wagner
Dominic Vella**

The ‘Sticky Elastica’: Delamination blisters beyond small deformations

TILL J. W. WAGNER¹ and DOMINIC VELLA²

¹ *Department of Applied Mathematics and Theoretical Physics, University of Cambridge, Wilberforce Rd, Cambridge, CB3 0WA, UK*

² *OCCAM, Mathematical Institute, 24-29 St Giles’, Oxford, OX1 3LB, UK*

PACS 62.20.mq – Buckling
PACS 68.35.Np – Adhesion

Abstract – We consider the form of an elastic loop adhered to a rigid substrate: the ‘sticky Elastica’. In contrast to previous studies of the shape of delamination ‘blisters’, the theory developed accounts for deflections with large slope (i.e. geometrically nonlinear). Starting from the classical Euler Elastica we provide numerical results for the dimensions of such blisters for a variety of end-end confinements and develop asymptotic expressions that reproduce these results well up to the point of self-contact. Interestingly, we find that the width of such blisters does not grow monotonically with increased confinement. Our theoretical predictions are confirmed by simple desktop experiments and suggest a new method for the measurement of the *elastocapillary length* for deformations that cannot be considered small.

Introduction. – Delamination blisters are often the undesired consequence of an adhesive film placed imperfectly on a substrate. They are the nemesis of anyone trying to wrap Christmas presents using sticky tape and regularly frustrate smartphone users who want to put a protective film on their phone screen. Blisters appear when an adhered film is subject to an in-plane compressive strain relative to the substrate. Such a strain can result from a differential compression (e.g. due to heating) or because of a mismatch between substrate and film geometries [1–4]. Even small mismatches can give rise to significant blisters, which can, in turn, greatly affect the functionality of the adhering film in applications from protective coatings to the conduction characteristics of Few Layer Graphene sheets [5–7].

Historically, delamination blisters have found use as a simple means of measuring the strength of adhesion between two materials, a series of methods known as *blister tests* [8–11]. However, more recently, and in spite of some of the negative connotations of delamination it has been proposed that partial delamination and buckling of thin adhesive sheets can be intentionally integrated into the design of flexible electronic devices [12–15]. In these devices, the conducting components are only adhered to the substrate in some regions and not others; this ‘blistered’ shape allows them to accommodate the flexure of

the substrate without deforming plastically. In current flexible electronic applications the form of these blisters is controlled by patterning the substrate with a periodic variation in adhesive strength. However, such techniques may suffer from the spontaneous formation of delamination blisters with a well-defined size [3]; understanding the size and form of such blisters is important since their characteristic curvature can damage the conducting components [12, 16].

While the formation of delamination blisters is a classical problem, previous analyses have focussed on the limit of blisters with a small slope (small deformations). However, in many new applications, this restriction is inappropriate. In this Letter, therefore, we consider the problem without the restriction of small slopes — we consider a single blister allowing for the possibility of large slopes (i.e. large deformations). Using a combination of numerical, asymptotic and experimental techniques we show how the results of previous small deformation analyses may be altered to take into account these large deformations and suggest how experimental data should be analysed to make use of our results.

Theory. – We consider an incompressible elastic sheet, resting on a semi-infinite, rigid substrate. The sheet is subjected to an in-plane compression Δl which

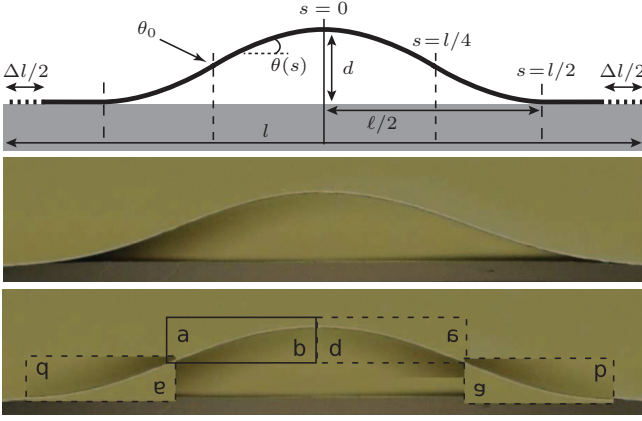


Fig. 1: The ‘sticky Elastica’. *Top*: schematic of a thin sheet resting on a substrate and subject to an end-end compression Δl . The result is a blister with arc-length l and dimensions d and ℓ . *Centre*: Experimental blister ($\ell_{ec} \approx 0.76$ cm), with $\Delta l = 0.03$ cm ($\Delta L \approx 0.04$), leading to $d = 0.17$ cm, $\ell = 1.16$ cm, ($\delta \approx 0.22$, $\lambda \approx 1.53$). *Bottom*: Illustration of the four-fold symmetry of the Elastica; the image in the central panel is reconstructed by taking the segment $-l/4 < s < 0$, (solid frame) and rotating and reflecting to form the other images — inversions of **a**, **b** illustrate the different reflexions. Here the sheet thickness $h = 42$ μm .

results in a delamination blister of height d and width ℓ (figure 1). The rate of compression is assumed small such that the sheet is in static equilibrium at any point. The shape of the blister is defined by the intrinsic angle $\theta(s)$, (s being the arc-length) and a point on the blister has coordinates $[x(s), w(s)]$ where $dx/ds = \cos \theta$ and $dw/ds = \sin \theta$ arise from geometric considerations. The delaminated portion has an (unknown) arc-length l , so that the end-points of the delaminated regions are given by $s = \pm l/2$. The system is assumed to be symmetric around $s = 0$, since the sheet remains smooth, we must have that $\theta(\pm l/2) = \theta(0) = 0$.

We shall use a variational approach to derive the appropriate governing equation and boundary conditions. In this formulation of the problem, we consider the energy of the system to be composed of a contribution from the bending energy of the sheet and another term from the sheet-substrate adhesion energy, $\Delta\gamma$. (We neglect the effect of the weight of the delamination buckle for simplicity.) We must minimize this combined energy subject to the constraint of an imposed end-end displacement Δl . Supplementing the energy (measured relative to the flat, fully adhered, state) with a Lagrange multiplier to enforce this constraint, the problem reduces to the minimization of

$$U = \int_{-l/2}^{l/2} \frac{1}{2} B \theta_s^2 + \Delta\gamma \, ds - \alpha \left[l - \Delta l - \int_{-l/2}^{l/2} \cos \theta \, ds \right]. \quad (1)$$

Here the first term represents the bending energy of the sheet, which has thickness h , Young’s modulus E

and Poisson ratio ν so that the bending stiffness $B = Eh^3/12(1 - \nu^2)$. The second term represents the adhesive penalty per unit length due to delamination. Here, $\Delta\gamma = \gamma_{sv}^{(\text{sheet})} + \gamma_{sv}^{(\text{substrate})} - \gamma_{ss}$, where γ_{sv} represents the solid-vapour surface energy and γ_{ss} the solid-solid energy for the sheet-substrate interface [17]. Generally, delamination is composed of fracture in a combination of modes I and II. The interfacial energy $\Delta\gamma$ is therefore a function of the relative amounts of each mode present in a given scenario. However, for blisters much larger than the thickness of the sheet, this fraction is independent of shape and so $\Delta\gamma$ may be assumed constant [18].

Using the Calculus of Variations allows us to determine equations for the shape of the delaminated blister, $\theta(s)$, and the length of the delaminated portion, l , that extremize the functional U given in (1). The requirement that $\delta U/\delta \theta = 0$ yields the classical Elastica equation for a free sheet that experiences a constant compressive stress T [19, 20]:

$$B\theta_{ss} = -T \sin \theta, \quad (2)$$

where the Lagrange multiplier $\alpha \rightarrow -T$. The requirement that $\delta U/\delta l = 0$ yields a condition on the curvature at contact [17, 18, 21, 22]

$$\theta_s(\pm l/2) = \sqrt{2}/\ell_{ec}, \quad (3)$$

where $\ell_{ec} = (B/\Delta\gamma)^{1/2}$ is the *elasto-capillary* length of the system [23].

We shall see that it is possible to make some analytical progress for the nonlinear equation (2). However, it is instructive to consider first the linearized problem, i.e. the small deformation limit. In this limit, $\theta(s) \ll 1$ and geometrical considerations give us that $\theta \sim d/\ell$ where d is the blister height and ℓ is the blister width. Since (3) gives us that $\theta_s \sim 1/\ell_{ec}$ and $\ell \approx l$ (for small deformations) we then have that $d/\ell^2 \sim 1/\ell_{ec}$. A more careful analysis shows that, in fact,

$$d/\ell^2 \approx \frac{1}{2^{1/2}\pi^2} \ell_{ec}^{-1}. \quad (4)$$

Referring to the quantity d/ℓ^2 as the typical curvature of the blister we see that, for small deformations at least, the typical curvature is a constant multiple of ℓ_{ec}^{-1} , independently of the dimensions of the blister [3, 4]. This result is therefore a useful simple method for measuring the elasto-capillary length of a system. The question arises, however, of how this result is modified for blisters beyond the small deformation limit? On dimensional grounds d/ℓ^2 must still scale like ℓ_{ec}^{-1} but, as we shall see, the aspect ratio d/ℓ also plays a role.

To facilitate our analysis, we first non-dimensionalize the system by letting $\tau = T/\Delta\gamma$, $\delta = d/\ell_{ec}$, $\lambda = \ell/\ell_{ec}$, $S = s/\ell_{ec}$, $L = l/\ell_{ec}$, etc.. The Elastica equation (2) then becomes $\theta_{SS} = -\tau \sin \theta$, with boundary condition $\theta_S(\pm L/2) = \sqrt{2}$. This can be integrated once to give

$$\theta_S^2 = 2 \frac{\cos \theta - \cos \theta_0}{1 - \cos \theta_0}, \quad (5)$$

where θ_0 is defined as the angle at which the curvature vanishes, i.e. the maximum value of θ within the sheet. By symmetry, we have that $\theta(-L/2) = \theta(0) = \theta(L/2) = 0$. The angle θ must therefore increase from 0 at $S = -L/2$ up to θ_0 and subsequently decrease from θ_0 to match $\theta = 0$ at $S = 0$. The symmetry of the problem therefore dictates that the inflection point $\theta_S = 0$ must occur at $S = \pm L/4$ so that

$$\theta_S = \sqrt{2} \left(\frac{\cos \theta - \cos \theta_0}{1 - \cos \theta_0} \right)^{1/2} \times \begin{cases} -1, & 0 \leq |S| < L/4, \\ +1, & L/4 \leq |S| \leq L/2. \end{cases} \quad (6)$$

We note that this requires that the blister is not only symmetric around $S = 0$ but, further, that the segment $L/4 < |S| < L/2$ is a rotation by 180° of the segment $0 < |S| < L/4$. This rotational and reflectional symmetry is illustrated in figure 1.

To make further progress requires the determination of the unknown angle θ_0 . To do this requires a relationship between the compression applied, ΔL , and θ_0 . Using the symmetry of the problem just discussed, we have that $\Delta L = 4 \int_0^{L/4} (1 - \cos \theta) dS$. Making use of the substitution $dS = d\theta/\theta_S$ and integrating from $\theta = 0$ to $\theta = \theta_0$, we find that:

$$\Delta L = 2^{5/2} (1 - \cos \theta_0) (\text{EF}[\mathbf{q}] - \text{EE}[\mathbf{q}]), \quad (7)$$

where $\mathbf{q} = (\frac{\theta_0}{2}, \csc^2 \frac{\theta_0}{2})$, and $\text{EF}[\dots]$ and $\text{EE}[\dots]$ are the Elliptical Integrals of First and Second Kind, respectively [24]. The expression (7) in principle allows us to obtain the maximum angle as a function of end-to-end compression, $\theta_0 = \theta_0(\Delta L)$, numerically. Once θ_0 is determined, it is a simple matter to calculate the dimensions of the blister as

$$\begin{aligned} \delta &= \int_{-L/2}^0 \sin \theta dS = 2^{3/2} (1 - \cos \theta_0), \\ \lambda &= \int_{-L/2}^{L/2} \cos \theta dS = \\ &2^{5/2} \{ (1 - \cos \theta_0) \text{EE}[\mathbf{q}] + \cos \theta_0 \text{EF}[\mathbf{q}] \}. \end{aligned} \quad (8)$$

Plots of the (numerically determined) evolution of the blister dimensions with increasing compression are given for $\lambda = \lambda(\Delta L)$ in fig. 3 and for $\delta = \delta(\Delta L)$ in fig. 4.

The shape of the blister $[X(S), W(S)]$ can also be determined using analogous integrals, and compared with experimental results (see figure 2). We also find that at a compression, $\Delta L^* \approx 8.71949$ ($\lambda^* \approx 1.55502$) the sheet comes into self-contact, forming a perfect ‘S’ shape.

Asymptotic Considerations. – The asymptotic result in (4) may be found by considering the leading order behaviour. However, it is possible to do better by retaining higher order terms in the θ_0 power series expansions of δ , λ and ΔL . By eliminating θ_0 in favour of ΔL we find that [17]

$$\delta = 2\sqrt{2} \left(\frac{\Delta L}{\pi} \right)^{2/3} - \frac{1}{2\sqrt{2}} \left(\frac{\Delta L}{\pi} \right)^{4/3} + \dots, \quad (9)$$

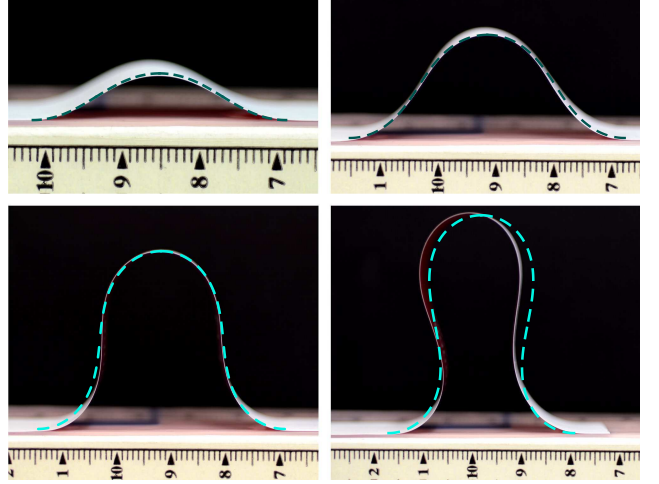


Fig. 2: The ‘sticky Elastica’ for $\Delta L = 0.18, 1.12, 3.25, 5.63$, ($\ell_{ec} = 1.35$ cm). In each case the theoretical prediction obtained using the experimentally measured value of Δl gives a good account of the experimentally observed blister shape (dashed curves). Here the sheet thickness $h = 0.72 \mu\text{m}$, corresponding to black triangles in figures 3-5.

$$\lambda = 2\pi^{2/3} \Delta L^{1/3} - \frac{7}{8} \Delta L + \dots \quad (10)$$

The first and second order asymptotics for $\lambda(\Delta L)$ and $\delta(\Delta L)$ are shown in figures 3 and 4, respectively. These demonstrate that, although only strictly being valid for $\Delta L \ll 1$, the two-term expansion compares extremely well with the numerical results even for $\Delta L \approx 7$, i.e. close to self-contact. We also note that the evolution of $\lambda(\Delta L)$ is non-monotonic (see fig. 3), decreasing for $\Delta L \gtrsim 64\pi/21^{3/2} \approx 2.0894$. While the asymptotic expression for δ likewise predicts a maximum height this only occurs for $\Delta L \approx 8\pi$, which is far beyond the point of self contact, ΔL^* (and hence is not physically realizable).

It is interesting to observe that, except for very small compressions ($\Delta L \lesssim 0.3$), the dependence of blister width on ΔL is relatively weak; we therefore propose that, as a rule of thumb, $\lambda \approx 3\ell_{ec}$. This result provides a quick way to get a rough estimate for the elasto-capillary length by looking just at the typical width of the blisters in a system. This gives further justification to the assumption that the blister width is roughly constant in delamination buckling, an assumption often called upon in previous work [18].

Using the asymptotic results from (9)-(10), we can return to the question of central interest here: how does the typical curvature d/ℓ^2 relate to the elastocapillary length? We find that the typical curvature can be expressed simply by eliminating ΔL in favour of δ/λ , the aspect ratio of the blister:

$$\frac{\delta}{\lambda^2} = \frac{1}{\sqrt{2}\pi^2} + \frac{3}{8\sqrt{2}} \left(\frac{\delta}{\lambda} \right)^2 - \dots \quad (11)$$

Thus, in the limit of small blisters we recover the result (4). However, as δ/λ increases the typical curvature grows

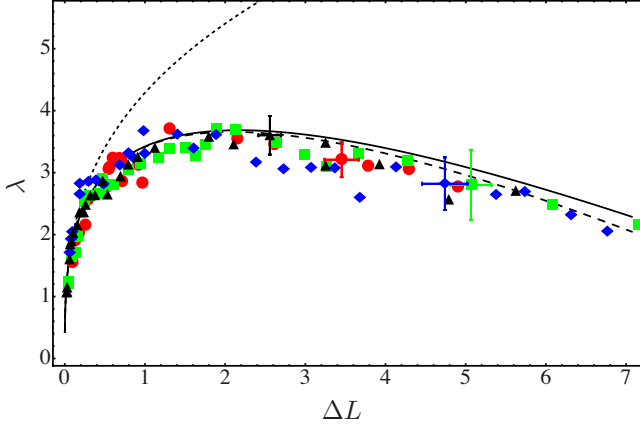


Fig. 3: Horizontal blister dimension, λ , as a function of the compression ΔL . The full numerical solution (solid black curve) is partially captured by the first order asymptotics (dotted). The second order asymptotic approximation (10) (dashed) gives a much better prediction and explains the non-monotonic behaviour. Points refer to experimental results obtained with different thickness sheets: $h_1 = 52\mu\text{m}$ (●), $h_2 = 42\mu\text{m}$ (■), $h_3 = 41\mu\text{m}$ (◆) and $h_4 = 70\mu\text{m}$ (▲). All lengths are non-dimensionalized by ℓ_{ec} , determined using the method described later.

roughly quadratically. The asymptotic relationship (11) agrees with the results of numerical calculations, as, together with the numerical results from (8) are shown in fig. 5.

Experiments. — The preceding theoretical analysis was tested using a set of macroscopic desktop experiments at a macroscopic scale. We used plastic sheets of different thicknesses adhered to tacky rubber surfaces (fabricated from Zhermack dental polymer). The sheets used were uniform strips of adhesive tape (thickness $h_1 = 52\mu\text{m}$, red circles in figures 3–5) and other thin elastic sheets without an adhesive coating, which were obtained from the labels of commonly available drink bottles (Aquafina, $h_2 = 42\mu\text{m}$, green squares; Copella, $h_3 = 41\mu\text{m}$, blue diamonds; and Vitamin Water $h_4 = 70\mu\text{m}$, black triangles in figures 3–5). The Young’s modulus of these sheets was measured to be $E = 0.7 \pm 0.1$ GPa using the deflection of the sheets under their own weight.

For the adhesion experiments described here, the sheets were cut into strips of width 1 cm and length 10 cm. The ends of these strips were then brought together by a distance Δl and the band then brought into contact with the substrate. Upon deposition the strip was forced into adhesion beyond its equilibrium state by applying pressure over almost the entire strip (missing out the central blistered part and avoiding the plastic deformations that occur for very high curvatures). Once the external pressure is removed, the strip spontaneously deadheres until reaching an equilibrium state in which the length of its deadhered portion, l , is well-defined, as shown in figure

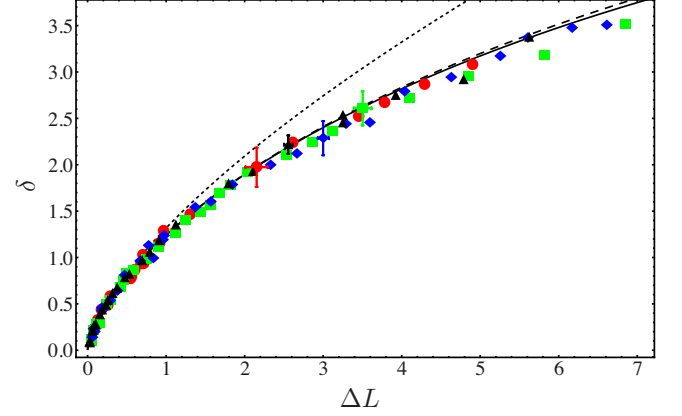


Fig. 4: Vertical blister dimension, δ , as a function of the compression ΔL . Shown are numerical solution (solid black curve), first order (dotted) and second order asymptotics (9) (dashed). Points refer to different thickness sheets: $h_1 = 52\mu\text{m}$ (●), $h_2 = 42\mu\text{m}$ (■), $h_3 = 41\mu\text{m}$ (◆) and $h_4 = 70\mu\text{m}$ (▲). All lengths are non-dimensionalized by ℓ_{ec} .

2. The results of experiments performed in this way were robust and reproducible.

The dimensions d and ℓ of the blisters in equilibrium were measured for a range of the end-end compression Δl . A comparison of experimental and theoretical predictions is given in figures 3–5. To plot these in dimensionless form the elastocapillary length for each strip-substrate pair had to be determined. This was done by plotting the dimensional values of d/ℓ^2 against the dimensionless quantity $1/\sqrt{2\pi^2} + (3/8\sqrt{2})(d/\ell)^2$ — eqn. (11) leads us to expect that such a plot should yield a straight line with slope $1/\ell_{ec}$. Such a plot is shown in figure 5 (inset) and demonstrates the expected linear behaviour. We therefore believe that this method represents an effective method for determining the elastocapillary length in scenarios where the aspect ratio d/ℓ is not small. We find for the adhesive tape $\ell_{ec}^{(1)} = 0.62$ cm and for the non-adhesive tapes $\ell_{ec}^{(2)} = 0.76$ cm, $\ell_{ec}^{(3)} = 0.64$ cm and $\ell_{ec}^{(4)} = 1.35$ cm. From this we infer for the adhesive tape $\Delta\gamma^{(1)} \simeq 0.25$ Jm⁻² and for the non-adhesive tapes $\Delta\gamma^{(2-4)} \simeq 0.08 - 0.13$ Jm⁻². This is comparable to values obtained in similar studies [3].

The agreement between theory and experiment shown in fig. 3–5 seems to be reasonably robust given the relative difficulty in measuring the exact blister width ℓ (rather than blister height d , which is much easier to measure). This is particularly important in figure 5, due to the ℓ^{-2} dependence of the typical curvature.

Conclusions. — In this letter we have presented numerical results for the shape and dimensions of delamination blisters allowing for the possibility that the slope of the blister may not be small. An asymptotic analysis yielded simple expressions for the dimensions of the blisters, which are in excellent agreement with numerical

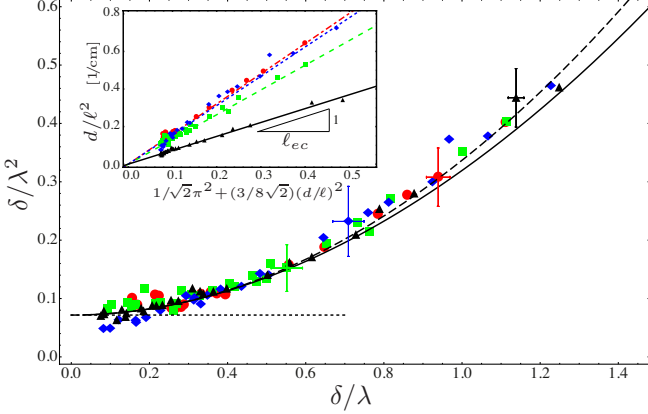


Fig. 5: Dimensionless typical curvature of blisters δ/λ^2 as a function of the aspect ratio δ/λ . Shown are full numerical solution, (solid black), first order (dotted) and second order asymptotic approximations (11), (dashed). Points refer to different thickness sheets: $h_1 = 52\mu\text{m}$ (\bullet), $h_2 = 42\mu\text{m}$ (\blacksquare), $h_3 = 41\mu\text{m}$ (\blacklozenge) and $h_4 = 70\mu\text{m}$ (\blacktriangle). *Inset*: Determination of the elastocapillary length, ℓ_{ec} for the four sets of experiments discussed. The straight lines represent best fits to the raw data. The slope of these lines provides estimates for the quantity $1/\ell_{ec}$. All lengths are non-dimensionalized by ℓ_{ec} .

results up to the point of self-contact. These asymptotic results also enabled us to propose a straight-forward way to estimate the strength of adhesion based on the geometry of delamination blisters beyond the limit of small deformations. We tested this technique with a series of simple table-top experiments obtaining good agreement between experiment and theory with a single fitting parameter: the elastocapillary length ℓ_{ec} , which relates the bending rigidity of the film and the adhesive energy.

Our study was motivated by the controlled use of delamination in technologies at small scales, most notably in flexible electronics. In these situations, the deformation of the delaminated components is often not small and so we expect that our results would be of use in such applications, albeit provided that a simple adhesion is used, rather than the patterning that is currently common [12]. In our analysis, we have assumed that there is no relative motion between strip and substrate. In reality, this can be achieved in two ways: (i) the sheet is confined *before* it is brought in contact with the rigid substrate (as in the experiments presented here) or (ii) the (relatively stiff) strip is initially flat and adhered to a compressible substrate. If the *entire* strip-substrate system is then compressed, the strip is forced to buckle out of plane and delaminate from the substrate forming a delamination blister. For our analysis to be applicable to this latter case, we require that the surface energy decrease due to the decrease in substrate surface energy in compression is small, i.e. that $\gamma_{sv} \ll \gamma_{ss}$ [17].

The main difference to canonical studies of delamination is that the width of the blister is not fixed *a priori* but is rather determined by a balance between bending and

adhesive forces at a fixed compression Δl . Nevertheless, our analysis shows that, in fact, as the compression is increased the preferred size of this blister changes only very slightly.

An important feature of blisters in flexible electronic applications is that the buckled components should retain a sufficiently small curvature that they do not deform plastically under repeated flexing. Here, we assume that this condition is satisfied provided that the stress within the beam, σ , does not reach the yield stress, σ_y . From linear elasticity theory, the maximum bending stress within a sheet occurs at the surfaces $z = \pm h/2$ of the sheet. Therefore if the sheet is deformed to have a maximum curvature $|\theta_s|_{\text{Max}}$ then $\sigma_{\text{Max}} = Eh|\theta_s|_{\text{Max}}/2(1-\nu^2)$ [25] and we have that no failure will occur provided that

$$\sigma_y > \sigma_{\text{Max}} = \frac{Eh}{2(1-\nu^2)}|\theta_s|_{\text{Max}}. \quad (12)$$

However, for the sticky elastica, our analysis has shown that the maximum curvature occurs at $s = 0, \pm l/2$ and has value $|\theta_s|_{\text{Max}} = \sqrt{2}/\ell_{ec}$, see (3). Buckling will therefore occur without plastic deformation provided that

$$\frac{\sigma_y^2 h}{E\Delta\gamma} > \frac{6}{1-\nu^2}, \quad (13)$$

i.e. provided that the thickness is large enough for given material properties, or provided the substrate-strip adhesion is sufficiently weak. We note that this result is precisely the same as that derived previously from linear considerations [3] but applies independently of the degree of compression, since the maximum curvature is given solely by the elastocapillary length ℓ_{ec} . In other words, the sheet is no more likely to fail for larger compressions than for the initial delamination event – if it survives the original deformation it can safely be compressed further.

This publication is based on work supported in part by Award No. KUK-C1-013-04, made by King Abdullah University of Science and Technology (KAUST). TJWW is supported by EPSRC.

REFERENCES

- [1] GIOIA G. and ORTIZ M., *Advances in applied mechanics*, **33** (1997) 119.
- [2] FAULHABER S., MERCER C., MOON M., HUTCHINSON J. and EVANS A., *Journal of the Mechanics and Physics of Solids*, **54** (2006) 1004.
- [3] VELLA D., BICO J., BOUDAUD A., ROMAN B. and REIS P. M., *Proc. Natl. Acad. Sci. USA*, **106** (2009) 10901.
- [4] AOYANAGI Y., HURE J., BICO J. and ROMAN B., *Soft Matter*, **6** (2010) 5720.
- [5] KIM E.-A. and CASTRO NETO A. H., *EPL*, **84** (2008) 57007.
- [6] SCHNIEPP H., KUDIN K., LI J., PRUDHOMME R., CAR R., SAVILLE D. and AKSAY I., *ACS nano*, **2** (2008) 2577.
- [7] LI Z., CHENG Z., WANG R., LI Q. and FANG Y., *Nano letters*, **9** (2009) 3599.

- [8] JENSEN H. M., *Eng. Fracture Mechanics* , **40** (1991) 475.
- [9] WAN K., *The Journal of Adhesion* , **70** (1999) 209.
- [10] CHOPIN J., VELLA D. and BOUDAUD A., *Proc. R. Soc. A* , **464** (2008) 2887.
- [11] KOENIG S., BODDETI N., DUNN M. and BUNCH J., *Nature Nanotechnology* , **6** (2011) 543.
- [12] SUN Y., CHOI W. M., JIANG H., HUANG Y. Y. and ROGERS J. A., *Nature Nanotech.* , **1** (2006) 201.
- [13] KHANG D., ROGERS J. and LEE H., *Advanced Functional Materials* , **19** (2009) 1526.
- [14] ROGERS J. A., SOMEYA T. and HUANG Y., *Science* , **327** (2010) 1603.
- [15] CHENG H., WU J., LI M., KIM D., KIM Y., HUANG Y., KANG Z., HWANG K. and ROGERS J., *Applied Physics Letters* , **98** (2011) 061902.
- [16] CHEN Z., COTTERELL B. and WANG W., *Eng. Fract. Mech.* , **69** (2002) 597.
- [17] (See Supplementary Information at ...).
- [18] HUTCHINSON J. and SUO Z., *Advances in applied mechanics* , **29** (1992) 191.
- [19] LOVE A., *A treatise on the mathematical theory of elasticity* (at the University Press) 1920.
- [20] AUDOLY B. and POMEAU Y., *Elasticity and geometry* (World Scientific Pub Co Inc) 2000.
- [21] LANDAU L. D. and LIFSHITZ E. M., *The Theory of Elasticity* (Pergamon) 1970.
- [22] MAJIDI C., *Mech. Res. Comm.* , **34** (2007) 85.
- [23] BICO J., ROMAN B., MOULIN L. and BOUDAUD A., *Nature* , **432** (2004) 690.
- [24] ABRAMOWITZ M. and STEGUN I. A., *Handbook of Mathematical Functions with Formulas, Graphs, and Mathematical Tables* (Dover, New York) 1964.
- [25] MANSFIELD E. H., *The Bending and Stretching of Plates* (Cambridge University Press) 1989.

RECENT REPORTS

12/20	Multiple equilibria in a simple elastocapillary system	Taroni Vella
12/21	Multiphase modelling of vascular tumour growth in two spatial dimensions	Hubbard Byrne
12/22	Chebfun and Numerical Quadrature	Hale Trefethen
12/23	Moment-based formulation of NavierMaxwell slip boundary conditions for lattice Boltzmann simulations of rarefied flows in microchannels	Reis Dellar
12/24	Correspondence between one- and two-equation models for solute transport in two-region heterogeneous porous media	Davit Wood Debenest Quintard
12/25	Rolie-Poly fluid flowing through constrictions: Two distinct instabilities	Reis Wilson
12/26	Age related changes in speed and mechanism of adult skeletal muscle stem cell migration	Collins-Hooper Woolley Dyson Patel Potter Baker Gaffney Maini Dash Patel
12/27	The interplay between tissue growth and scaffold degradation in engineered tissue constructs	ODEa Osborne El Haj Byrne Waters
12/28	Non-linear effects on Turing patterns: time oscillations and chaos.	Aragon Barrio Woolley Baker Maini
12/29	Colorectal Cancer Through Simulation and Experiment	Kershaw Byrne Gavaghan Osborne
12/30	A theoretical investigation of the effect of proliferation and adhesion on monoclonal conversion in the colonic crypt	Mirams Fletcher Maini Byrne
12/31	Convergent evolution of spiny mollusk shells points to elastic energy minimum	Chirat Moulton Shipman Goriely

12/34	The sensitivity of Graphene 'Snap-through' to substrate geometry	Wagner Vella
12/35	The physics of frost heave and ice-lens growth	Peppin Style
12/36	Finite Element Simulation of Dynamic Wetting Flows as an Interface Formation Process	Sprittles Shikhmurzaev
12/37	The Dynamics of Liquid Drops and their Interaction with Solids of Varying Wettabilities	Sprittles Shikhmurzaev
12/38	Dispersal and noise: Various modes of synchrony in ecological oscillators	Bressloff Lai
12/39	Boundary conditions for free surface inlet and outlet problems	Taroni Breward Howell Oliver
12/40	A Branch and Bound Algorithm for the Global Optimization of Hessian Lipschitz Continuous Functions	Fowkes Gould Farmer
12/41	The Orthogonal Gradients Method: a Radial Basis Functions Method for Solving Partial Differential Equations on Arbitrary Surfaces	Piret
12/42	Squeeze-Film Flow in the Presence of a Thin Porous Bed, with Application to the Human Knee Joint	Knox Wilson Duffy McKee
12/43	Gravity-driven draining of a thin rivulet with constant width down a slowly varying substrate	Paterson Wilson Duffy

Copies of these, and any other OCCAM reports can be obtained from:

**Oxford Centre for Collaborative Applied Mathematics
Mathematical Institute
24 - 29 St Giles'
Oxford
OX1 3LB
England
www.maths.ox.ac.uk/occam**